

See discussions, stats, and author profiles for this publication at: <https://www.researchgate.net/publication/224184961>

# High pressure stability of bismuth sillenite: A Raman spectroscopic and x-ray diffraction study

ARTICLE *in* JOURNAL OF APPLIED PHYSICS · NOVEMBER 2010

Impact Factor: 2.18 · DOI: 10.1063/1.3496659 · Source: IEEE Xplore

---

CITATIONS

5

---

READS

15

3 AUTHORS, INCLUDING:



Alka Garg

Bhabha Atomic Research Centre

58 PUBLICATIONS 263 CITATIONS

SEE PROFILE

# High pressure stability of bismuth sillenite: A Raman spectroscopic and x-ray diffraction study

Rekha Rao,<sup>1,a)</sup> Alka B. Garg,<sup>2</sup> and T. Sakuntala<sup>3</sup>

<sup>1</sup>*Solid State Physics Division, Bhabha Atomic Research Centre, Mumbai 400 085, India*

<sup>2</sup>*High Pressure & Synchrotron Radiation Physics Division, Bhabha Atomic Research Centre, Mumbai 400 085, India*

<sup>3</sup>*Department of Atomic Energy, Strategic Planning Group, Mumbai 400 001, India*

(Received 28 July 2010; accepted 29 August 2010; published online 20 October 2010)

High pressure behavior of the compound  $\text{Bi}_{12}\text{SiO}_{20}$  is investigated using *in situ* Raman spectroscopic and synchrotron-based angle dispersive x-ray diffraction techniques. Results indicate that the compound remains stable in the ambient pressure cubic structure up to 26 GPa. From the structural studies, bulk modulus  $B_0$ , and its pressure derivative  $B'$  of  $\text{Bi}_{12}\text{SiO}_{20}$  are evaluated to be 36 GPa and 16.7 GPa, respectively. Mode Grüneisen parameters of various Raman active modes of  $\text{Bi}_{12}\text{SiO}_{20}$  are also reported. The stability of  $\text{Bi}_{12}\text{SiO}_{20}$  at high pressure is discussed in the light of the pressure-induced amorphization reported in bismuth-orthosilicate ( $\text{Bi}_4\text{Si}_3\text{O}_{12}$ ) and -orthogermanate. Comparison of the observed phonon behavior with that reported for  $\text{Bi}_4\text{Si}_3\text{O}_{12}$  reveals that two of the Raman modes in  $\text{Bi}_4\text{Si}_3\text{O}_{12}$  have negative pressure dependencies clearly indicating dynamic instability while  $\text{Bi}_{12}\text{SiO}_{20}$  does not show any signatures of zone-center instabilities. © 2010 American Institute of Physics. [doi:10.1063/1.3496659]

## I. INTRODUCTION

The oxides  $\text{Bi}_2\text{O}_3$  and  $\text{SiO}_2/\text{GeO}_2$  are known to form silicates/germanates in different molar ratios such as  $\text{Bi}_2\text{SiO}_5$ ,  $\text{Bi}_2\text{Si}_3\text{O}_9$ ,  $\text{Bi}_4\text{Si}_3\text{O}_{12}$ , and  $\text{Bi}_{12}\text{SiO}_{20}$ . Among these, the compound  $\text{Bi}_4\text{Si}_3\text{O}_{12}$  (bismuth orthosilicate) and  $\text{Bi}_{12}\text{SiO}_{20}$  (bismuth sillenite) have several interesting properties such as large value of dielectric constant, piezoelectric and elasto-optic coefficients, very high refractive index and hence are technologically important.<sup>1,2</sup> These compounds belong to the family of lead-free piezoelectric materials which are of current interest.  $\text{Bi}_{12}\text{SiO}_{20}$  (BSO) is a member of the sillenite-class of compounds formed by  $(\text{Bi}_2\text{O}_3)_6$  and various metal oxides of type  $\text{MO}_2$  ( $M$ : Si, Ge, Ti, Mn) crystallizing in a cubic structure, of space group  $I23$ . Structure of the other class of compounds having the general formula  $\text{Bi}_4\text{M}_3\text{O}_{12}$  ( $M$ =Si, Ge, Ti), on the other hand, is dependent on the cation. For  $M$ =Si, Ge, the system is cubic, having a space group ( $I43d$ ) and for  $M$ =Ti, the compound crystallizes in monoclinic aurivillius structure.<sup>3</sup> Extensive structural studies have been carried out on both the classes of compounds with a view of understanding the origin of their piezoelectric properties, which are primarily related to the  $\text{MO}_4$  tetrahedron. Besides other interests, a wide variety of sillenites, including those formed with  $\text{M}'_2\text{O}_3$  ( $M'$ =Sc, Y, Nb, etc.), have been studied with a view to understand the structure of the mineral sillenite,  $\gamma\text{-Bi}_2\text{O}_3$ .

Studies on the high pressure behavior of BSO are relatively less. Earlier high pressure optical absorption studies on BSO reported an increase in absorption coefficient up to 1 GPa, which was attributed to the shift in defect level.<sup>4</sup> Present investigations on the high pressure behavior of BSO have interest from two aspects. Many of the tetrahedrally

coordinated silicate-based compounds have shown interesting phase transition behavior under the application of pressure, transforming to sixfold coordinated structures, and have been the subject of extensive experimental and theoretical studies.<sup>5</sup> While the silicate perovskites such as  $\text{CaSiO}_3$ ,  $\text{MgSiO}_3$ , etc., exhibit pressure induced amorphization during decompression,<sup>6</sup> spinels like  $\text{Fe}_2\text{SiO}_4$  and  $\text{Mg}_2\text{SiO}_4$  undergo disproportionation at high pressure-high temperature conditions.<sup>7</sup> Besides transition involving coordination changes, tetragonal silicates such as zircon and hafnon have been reported to undergo volume-reducing zircon to scheelite transition,<sup>8,9</sup> wherein the Si-coordination remains the same. These phases are known to have high bulk modulus,<sup>10</sup> and the postscheelite phases are predicted to be even harder. In the case of BSO, *abinitio* calculations<sup>11</sup> had predicted a bulk modulus of  $B_0=74.4$  GPa, which is quite low for a silicate, thus prompting the experimental study of the compressibility behavior of BSO.

The other aspect is the pressure induced amorphization (PIA) behavior. It may be mentioned that PIA has been reported in the parent compounds  $\text{SiO}_2/\text{GeO}_2$ ,<sup>12,13</sup> as well as in  $\text{Bi}_2\text{O}_3$  (Ref. 14) above 21 GPa. Under the application of pressure,  $\text{Bi}_4\text{Ge}_3\text{O}_{12}$  was reported to undergo PIA above 12 GPa irreversibly.<sup>15</sup> High pressure studies on  $\text{Bi}_4\text{Si}_3\text{O}_{12}$  revealed that it undergoes reversible amorphization above 16 GPa.<sup>16</sup> PIA was understood as arising due to kinetic hindrance of decomposition of  $\text{Bi}_4\text{Si}_3\text{O}_{12}$  into simpler oxides of lower volume. Similar condition was found to be satisfied in bismuth orthogermanate also;<sup>17</sup> however, for BSO, pressure-induced decomposition (PID) did not appear to be favorable from volume considerations,<sup>16</sup> thus it was conjectured that PIA also may not be expected. Interestingly, many of the framework-structured compounds that have relatively low compressibility such as compounds belonging to the tung-

<sup>a)</sup>Electronic mail: rekhar@barc.gov.in.

state, vanadate family have been found to exhibit structural transitions at rather moderate pressures and subsequently exhibit PIA.<sup>18,19</sup>

Structural stability of BSO is investigated at high pressure in view of the predicted low bulk modulus of BSO and a tendency for PIA/structural transitions in related compounds. We report the high pressure behavior of BSO up to 26 GPa investigated using *in situ* Raman spectroscopy and angle dispersive x-ray diffraction (ADXRD) measurements.

## II. EXPERIMENTAL DETAILS

Transparent single crystals of BSO were grown by the Czochralski method. Raman scattering measurements at high pressure were carried out from unoriented single crystal bits of BSO from inside a diamond anvil cell (DAC). A 4:1 methanol-ethanol mixture was used as pressure transmitting medium. Raman spectra were excited using 532 nm laser of power  $\sim 15$  mW. Scattered light was analyzed using a home built 0.9 m single monochromator, coupled with a super notch filter and detected by a cooled CCD (Andor Technology). Entrance slit was kept at  $50\text{ }\mu\text{m}$ , which gives a spectral band pass of  $3\text{ cm}^{-1}$ .

*In situ* high pressure x-ray diffraction (XRD) measurements were carried out at the powder XRD beam line of Elettra synchrotron source, Italy. The data was collected in ADXRD mode, in the transmission geometry. The sample-to-image plate (IP) distance was calibrated using  $\text{CeO}_2$  diffraction pattern. For high pressure measurements, finely powdered BSO along with copper as internal pressure marker, and methanol-ethanol mixture as pressure transmitting medium were loaded in a Mao-Bell-type DAC having diamond anvils of culets size  $\sim 400\text{ }\mu\text{m}$ . X-ray powder patterns at various pressures were collected using x-ray of wavelength  $0.688\text{ }\text{\AA}$  collimated to  $80\text{ }\mu\text{m}$  diameter. Images of the powder diffraction rings were read from the MAR345 IP detector with a resolution of  $100 \times 100$  pixel size. The images thus obtained were integrated using the program FIT2D (Ref. 20) GSAS for structural refinement.<sup>21</sup> X-ray powder patterns were collected up to 24 GPa.

## III. RESULTS AND DISCUSSIONS

### A. High pressure raman spectroscopy

BSO belongs to body centered cubic structure with space group  $I23$ . With one formula unit per primitive cell, group theoretical analysis predicts 40 Raman active modes distributed as  $8A+8E+24F$ .<sup>22</sup> Raman spectrum at ambient conditions agree with that of the reported, all the 20 reported<sup>1</sup> distinct Raman active modes could be observed at ambient conditions. The modes in the interval  $45\text{--}170\text{ cm}^{-1}$  are due to the lattice modes. The internal modes related to Bi-O and  $\text{SiO}_4$  tetrahedra appear between  $200\text{--}850\text{ cm}^{-1}$ . At high pressures, all the Raman active modes above  $90\text{ cm}^{-1}$  could be followed up to 26 GPa. Figure 1 shows Raman spectrum of BSO at various pressures. All the modes increase in frequency with increasing pressure. Around 12 GPa, in the low frequency region of Bi-O breathing modes, around  $210\text{ cm}^{-1}$ , two new modes appear as shown by arrows in Fig. 1(a). Above 12 GPa, the mode at around  $110\text{ cm}^{-1}$  be-

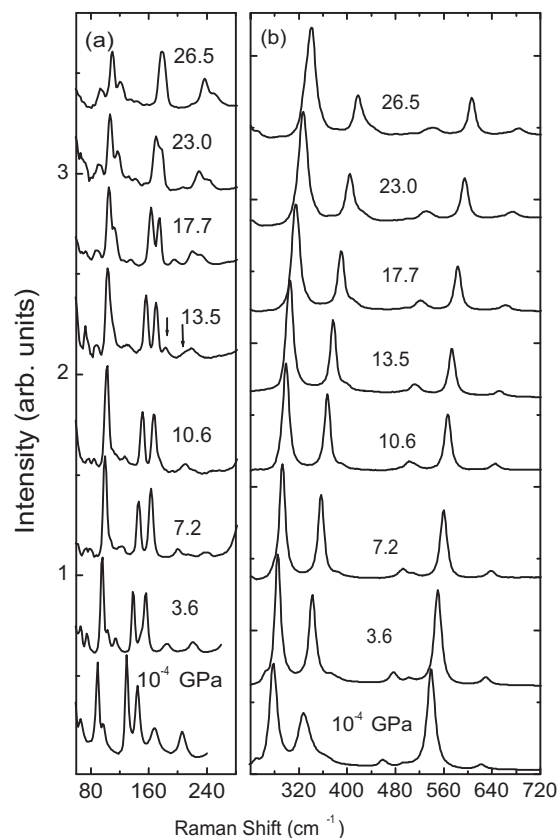


FIG. 1. (a) and (b) Raman spectra of BSO at various pressures. Arrows indicate the appearance of new peaks above 12 GPa.

longing to  $A$  symmetry increases in intensity. There is an overall redistribution of intensity in the region  $100\text{--}220\text{ cm}^{-1}$  above 12 GPa.

Figure 2 shows the pressure dependence of mode frequencies. Most of the Raman modes are noted to exhibit monotonic pressure dependence. Appearance of new modes

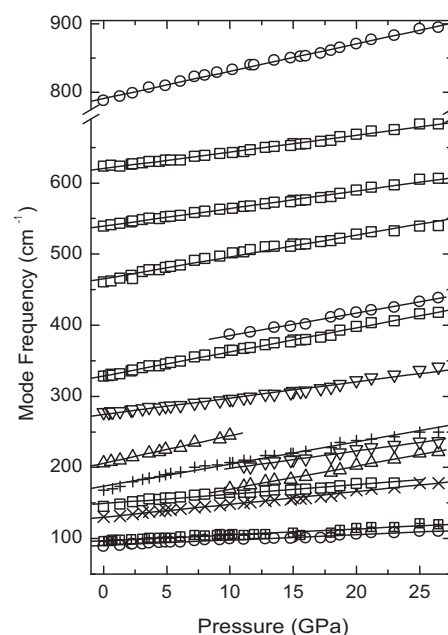


FIG. 2. Pressure dependence of mode frequencies in BSO. The solid lines are the least square fit to the data.

TABLE I. Ambient pressure phonon frequencies, their pressure derivatives, and mode Grüneisen parameters for various modes of BSO. Value of bulk modulus  $B_0=36$  GPa, obtained in the present studies is used for computing  $\gamma_i$ . The mode assignments are taken from Ref. 22. \* indicates the value of mode frequencies extrapolated to ambient pressure.

Mode symmetry	Frequency at 295 K (cm <sup>-1</sup> )	$d\omega/dP$ cm <sup>-1</sup> /GPa	$\gamma_i$
E	89	0.75	0.30
A	96	0.84	0.31
E	130	1.6	0.5
...	137*	3.2	0.84
A	145	1.33	0.32
A	168	3.13	0.65
...	175*	2.4	0.5
F	206	3.8	0.66
A	278	2.5	0.3
A	329	3.27	0.36
F	353*	3.17	0.32
E	465	3.1	0.24
A	539	2.5	0.17
E	623	2.33	0.14
A	788	3.2	0.15

and changes in relative intensities above 12 GPa may be due to a subtle transition around 12 GPa. Upon further increase in pressure, evolution of the spectrum was monotonous with no signatures of disorder up to 26 GPa. The intensity and the width of Raman modes in BSO remain intact indicating the crystalline phase is stable up to the highest pressure of 26 GPa investigated. The ambient phase Raman spectrum is recovered when the pressure is released. Table I shows the pressure dependencies of mode frequencies in BSO. In order to ascertain if the subtle changes around 12 GPa are due to a phase transition, *in situ* high pressure ADXRD experiments were carried out up to 24 GPa.

## B. High pressure x-ray diffraction

BSO crystallizes in cubic framework structure consisting of SiO<sub>4</sub> tetrahedra corner-linked to distorted BiO<sub>7</sub> polyhedra.<sup>23</sup> The MO<sub>4</sub> tetrahedral units ( $M$ : Si, Ge, Ti) in silenites are very close to the ideal tetrahedron.<sup>23</sup> The unit cell has Si atom at the origin and the body center (2a). Table II gives the typical atom position in BSO for the other atoms namely Bi and O. The bismuth and one of the oxygen (O1) are located in the general position (24f) while the other two oxygen atoms are located at the 8c positions, along the body diagonal. The oxygen atoms O3 are tetrahedrally coordinated

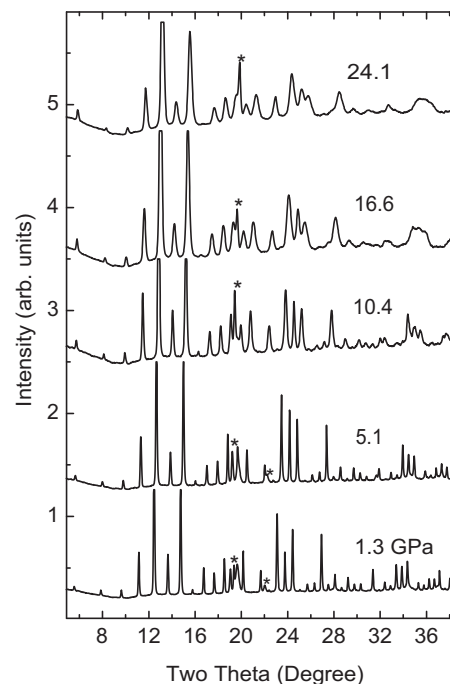


FIG. 3. Powder XRD pattern of Bi<sub>12</sub>SiO<sub>20</sub> at various pressures. \* indicate prominent diffraction peaks due to pressure marker. Intensities of some of the strong diffractions are clipped for clarity.

to the Si atom while O1 and O2 participate in forming the BiO<sub>7</sub> polyhedron. Five of the Bi–O distances lie in the range of 2.1–2.65 Å while two more Bi–O bond are of about 3.1 Å. The lattice parameter obtained by fitting the ambient pressure data  $a=10.14$  Å is in good agreement with that of the reported value of 10.10 Å.<sup>24</sup> Figure 3 shows the diffraction patterns at several high pressures. Evolution of the pattern is noted to be monotonic with increasing pressure. Above 10 GPa, it is observed that the peaks corresponding to higher theta value showed significant broadening. However, the data could be fitted to ambient cubic phase up to the highest pressure investigated (24.1 GPa). It may be noted that the broadening of the diffraction peaks in the low theta region is of lesser degree. Figures 4(a)–4(c) show some of the representative rietveld-refined XRD pattern at 1.3 GPa, 10.4 GPa, and 24.1 GPa, respectively. The  $R$  factors<sup>25</sup> of the refinements shown in Fig. 4 are given in Table II. Figure 5 shows the  $P$ - $V$  data for BSO up to 24.1 GPa. The data could be fitted to third order Birch Murnaghan equation of state,<sup>26</sup> given as

TABLE II. Refined structural parameters of Bi<sub>12</sub>SiO<sub>20</sub>; SG: I23,  $Z=2$ , at different pressures. Si atom is at (0,0,0); residuals (a) at  $P=1.3$  GPa:  $R_{wp}=0.047$ ,  $R_p=0.028$ ,  $R(F^2)=0.228$ ; (b) at  $P=10.4$  GPa:  $R_{wp}=0.043$ ,  $R_p=0.031$ ,  $R(F^2)=0.187$ , and (c) at  $P=24.1$  GPa:  $R_{wp}=0.046$ ,  $R_p=0.03$ ,  $R(F^2)=0.042$ , Ref. 25.

Atom	Site	$P=1.3$ GPa $a=10.0336(1)$ (Å)			$P=10.4$ GPa $a=9.7306(3)$ (Å)			$P=24.1$ GPa $a=9.4997(7)$ (Å)		
		x	y	z	x	y	z	x	y	z
Bi	24f	0.8237	0.6797	0.9850	0.8267	0.6766	0.9841	0.8294	0.6771	0.9882
Si	2a	0	0	0	0	0	0	0	0	0
O1	24f	0.890	0.726	0.482	0.842	0.766	0.503	0.866	0.740	0.525
O2	8c	0.787	0.787	0.787	0.801	0.801	0.801	0.785	0.785	0.785
O3	8c	0.094	0.094	0.094	0.150	0.150	0.150	0.113	0.113	0.113

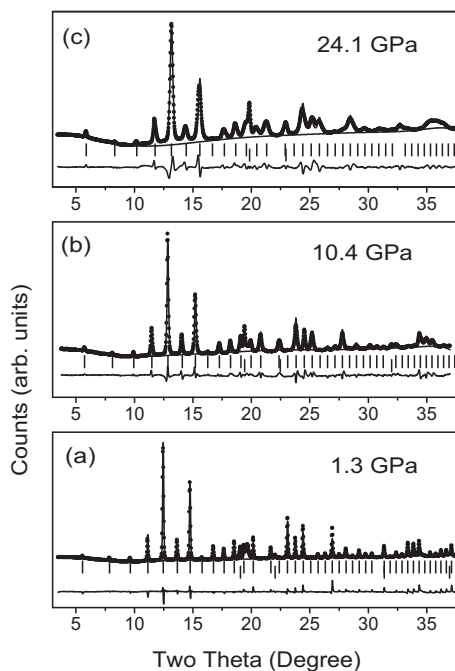


FIG. 4. Rietveld refined XRD pattern at (a) 1.3, (b) 10.4, and (c) 24.1 GPa. Upper tick marks indicate the peaks due to the sample and the lower tick marks denote those of the pressure calibrant, copper.

$$P = \frac{3}{2}B_0[(V_0/V)^{7/3} - (V_0/V)^{5/3}][1 - \frac{3}{4}(4 - B') \times \{(V_0/V)^{2/3} - 1\}],$$

where,  $B_0$  and  $V_0$  ( $1042.59 \text{ \AA}^3$ ) are the ambient pressure bulk modulus and volume, respectively;  $V$  is the volume at pressure  $P$ . Using the above relation, a value of 36 GPa was obtained for zero pressure bulk modulus  $B_0$  and 16.7 as its pressure derivative  $B'$ . The value of bulk modulus is much lower than the value of  $B_0 = 74.4 \text{ GPa}$  calculated by *ab initio* LDA calculations.<sup>11</sup> Interestingly, the value of  $B_0 = 58.9 \text{ GPa}$ ; obtained using the GGA approximation,<sup>11</sup> is closer to the experimentally obtained value of 36 GPa for BSO. Large value of the pressure derivative of bulk modulus,  $B'$  implies that under pressure the material progressively hardens with increasing pressure.<sup>27,28</sup>

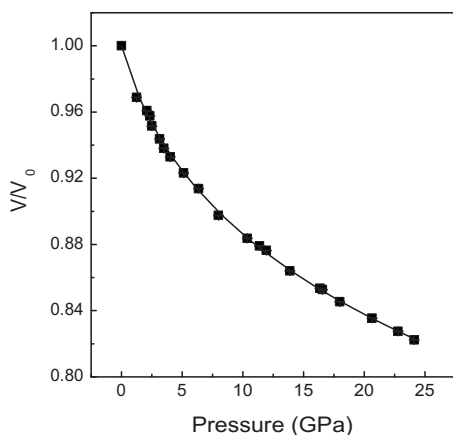


FIG. 5. Pressure-volume data for  $\text{Bi}_{12}\text{SiO}_{20}$ . Square symbols are experimental data points and solid line is the fitted data to the third order Birch-Murnaghan equation of state.

From the  $P$ - $V$  behavior it emerges that the cubic phase of BSO is stable up to the highest pressure reached in the present investigation, with no evidence for disorder setting-in. This further suggests that the new modes appearing in the Raman spectrum above 12 GPa are most likely due to the pressure dependencies of the line shapes of different Raman modes being different. As mentioned earlier, though PID/PIA was not expected in BSO from simple volume considerations, structural stability of the highly compressible cubic-BSO is unexpected. In an effort to understand the basic difference in stability between BSO and  $\text{Bi}_4\text{Si}_3\text{O}_{12}$ , phonon behavior in the two compounds was compared. Evolution of Raman spectrum in  $\text{Bi}_4\text{Si}_3\text{O}_{12}$  at high pressures showed that two of the lattice modes (at 202 and  $334 \text{ cm}^{-1}$ ) exhibit softening suggesting instability of the parent structure.<sup>16</sup> In the case of  $\text{Bi}_4\text{Ge}_3\text{O}_{12}$  also, two of the Raman modes at 203 and  $246 \text{ cm}^{-1}$  were reported to exhibit softening.<sup>15</sup> Table I shows the pressure dependence Raman mode frequencies and the Mode Grüneisen parameters of BSO. In contrast to the behavior of both  $\text{Bi}_4\text{Si}_3\text{O}_{12}$  and  $\text{Bi}_4\text{Ge}_3\text{O}_{12}$ , frequencies of all the Raman active modes increase with increasing pressure in BSO. While one-to-one comparison of the phonons in the two compounds is not meaningful as the compounds are different, there is no noticeable evidence of zone-center instability in the case of BSO. Pressure dependencies of most of the mode frequencies in BSO are found to be higher than those observed in  $\text{Bi}_4\text{Si}_3\text{O}_{12}$ .<sup>16</sup>

A class of high symmetry compounds known to have good stability under the application of high pressure is that of garnets. These also have framework structure and crystallize in cubic structure<sup>29–31</sup> and remain in the ambient pressure phase up to very high pressures. In the case of yttrium aluminum garnet,<sup>32</sup> it is observed that, the value of mode Grüneisen parameters  $\gamma_i$ , lies in a small range. The small range of  $\gamma_i$  indicates that the binding forces are of nearly same nature and comparable magnitude.<sup>32</sup> It may be noted that in BSO also, all the mode Grüneisen parameters are in a small range (0.14 to 0.84). In contrast, the mode Grüneisen parameters in orthosilicates, are noted to be widely different ( $-0.06$  to  $4.1$ ). However, most of the garnets have high bulk modulus;  $B_0 > 150 \text{ GPa}$ . Table III gives a list of compounds with cubic structure (at ambient conditions), their reported bulk modulus and high pressure behavior. Low bulk modulus has been noted in a few other framework structured materials crystallizing in cubic structure, such as  $\text{ZrW}_2\text{O}_8$  and related compounds.<sup>19</sup> Many of these compounds transform to lower symmetry phase at a moderate pressure, and subsequently amorphize under the application of pressure. A closer comparison of equation of state of BSO and other compounds like tungstates, reveals that the high pressure phases of tungstates continue to be soft,<sup>27</sup> i.e., very low or negative  $B'$  is noted in compounds that exhibit amorphization under pressure. In the light of such a trend, higher value of  $B'$  in BSO correlates well with the absence of any tendency for amorphization at high pressures suggesting that the compound progressively becomes harder at high pressures.



TABLE III. The structure, bulk modulus  $B_0$ , its derivative  $B'$ , and amorphization pressure  $P_A$  of some of the representative frame-work structured compounds that crystallize in cubic structure. \* indicates compounds for which  $B_0$  is obtained by fitting second order Birch–Murnaghan equation of state assuming  $B'$  to be 4.

Compound	Space group	$B_0$ (GPa)	$B'$	$P_A$ (GPa)
BSO	$I23$	36	16.7	No PIA up to 26 GPa
$\text{Bi}_4\text{Si}_3\text{O}_{12}$	$I\bar{4}3d$	230	NA	16
$\text{Bi}_4\text{Ge}_3\text{O}_{12}$	$I\bar{4}3d$	48	9	12
$\text{ZrW}_2\text{O}_8$ (Refs. 18 and 33)	$P2_13$	72.5	1.5	1.5
$\text{HfW}_2\text{O}_8$ (Ref. 34)	$P2_13$	82	NA	2.0
$\text{HfV}_2\text{O}_7$ (Ref. 19)	$Pa\bar{3}$	12.8	4*	Onset of PIA $\sim$ 5 GPa
$\text{ZrV}_2\text{O}_7$ (Ref. 19)	$Pa\bar{3}$	17.0	4*	4
$\text{ZrP}_2\text{O}_7$ (Ref. 19)	$Pa\bar{3}$	39	2.8	No PIA up to 20 GPa
garnet Pyrope	$Ia\bar{3}d$	199	4*	No PIA up to 28 GPa
$\text{Mg}_3\text{Al}_2(\text{SiO}_4)_3$ (Ref. 35)				
garnet Almandine	$Ia\bar{3}d$	189	4.2	No PIA up to 21GPa
$\text{Fe}_3\text{Al}_2(\text{SiO}_4)_3$ <sup>36</sup>				
Yttrium Al garnet	$Ia3d$	183.5	4*	No PIA 100 GPa
$\text{Y}_3\text{Al}_5\text{O}_{12}$ <sup>37,38</sup>				

## IV. CONCLUSION

High pressure behavior of bismuth sillenite ( $\text{Bi}_{12}\text{SiO}_{20}$ ) is investigated up to 26 GPa using *in situ* Raman spectroscopy and x-ray diffraction techniques. Results indicate that  $\text{Bi}_{12}\text{SiO}_{20}$  does not exhibit any phase transition up to 26 GPa. The bulk modulus and its derivative obtained by fitting third order Birch–Murnaghan equation of state are obtained to be  $B_0=36$  GPa  $B'=16.7$ , respectively. On comparing the phonon behavior of the highly compressible BSO with that of  $\text{Bi}_4\text{Si}_3\text{O}_{12}$ , signature of dynamic instability is clearly found in  $\text{Bi}_4\text{Si}_3\text{O}_{12}$  while in BSO there are no indications of at least zone-center instabilities. The stability of  $\text{Bi}_{12}\text{SiO}_{20}$  is explained on the basis of a comparison of its mode Grüneisen parameters with that of other related compounds. Comparison of the compression behavior of BSO with other frame-work structured compounds indicate that while those compounds that exhibit PIA have smaller values of  $B'$ , BSO is observed to have large value of  $B'$  correlating well with the absence of tendency for amorphization at high pressure.

## ACKNOWLEDGMENTS

Authors thank Dr. A. P. Roy for the gift of BSO single crystal. High pressure XRD experiments were done during the free time of proposal No. 2007570. We acknowledge the DST, India for travel support and Italian Government for hospitality at Elettra, Italy.

<sup>1</sup>B. Mihailova, M. Gospodinov, and L. Konstantinov, *J. Phys. Chem. Solids* **60**, 1821 (1999).

<sup>2</sup>M. Wintermantel and I. Biaggio, *Phys. Rev. B* **67**, 165108 (2003).

<sup>3</sup>A. D. Rae, J. G. Thompson, R. L. Withers, and A. C. Willis, *Acta Crystallogr. B* **46**, 474 (1990).

<sup>4</sup>T. Toyoda, H. Nakanishi, S. Endo, and T. Irie, *J. Appl. Phys.* **62**, 2012 (1987).

<sup>5</sup>W. H. Baur and A. A. Khan, *Acta Crystallogr. B* **27**, 2133–2139 (1971);

M. T. Dove, M. Gambhir, and K. D. Hammonds, *Phase Transitions* **58**, 121 (1996); D. M. Teter, R. J. Hemley, G. Kresse, and J. Hafner, *Phys. Rev. Lett.* **80**, 2145 (1998); G. Serghiou, R. Boehler, and A. J. Chopelas, *J. Phys. Condens. Matter* **12**, 849 (2000).

<sup>6</sup>M. Hemmati, A. Chizmeshya, G. H. Wolf, P. H. Poole, J. Shao, and C. A. Angell, *Phys. Rev. B* **51**, 14841 (1995).

<sup>7</sup>W. A. Bassett and L. Ming, *Phys. Earth Planet. Inter.* **6**, 154 (1972).

<sup>8</sup>E. Knittle and Q. Williams, *Am. Mineral.* **78**, 245 (1993); M. Marqués, M. Flórez, J. M. Recio, L. Gerward, and J. Staun Olsen, *Phys. Rev. B* **74**, 014104 (2006).

<sup>9</sup>B. Manoun, R. T. Downs, and S. K. Saxena, *Am. Mineral.* **91**, 1888 (2006).

<sup>10</sup>H. P. Scott, Q. Williams, and E. Knittle, *Phys. Rev. Lett.* **88**, 015506 (2001).

<sup>11</sup>H. Yao, L. Ouyang, and W. Ching, *J. Am. Ceram. Soc.* **90**, 3194 (2007).

<sup>12</sup>R. J. Hemley, A. P. Jephcoat, H. K. Mao, L. C. Ming, and M. H. Manghnani, *Nature (London)* **334**, 52 (1988).

<sup>13</sup>T. Yamanaka, T. Shibata, S. Kawasaki, and S. Kume, in *High Pressure Research: Application to Earth and Planetary Sciences*, edited by Y. Syono and M. H. Manghnani (Terrapub, Tokyo, 1992), p. 493.

<sup>14</sup>C. Chouinard and S. Desgreniers, *Solid State Commun.* **113**, 125 (1999).

<sup>15</sup>G. Zou, Z. Liu, L. Wang, Y. Zhao, Q. Cu, and D. Li, *Phys. Lett. A* **156**, 450 (1991).

<sup>16</sup>T. R. Ravindran, A. K. Arora, and R. Gopalakrishnan, *J. Phys.: Condens. Matter* **14**, 6579 (2002).

<sup>17</sup>A. K. Arora, T. Yagi, N. Miyajima, and R. Gopalakrishnan, *J. Phys.: Condens. Matter* **16**, 8117 (2004).

<sup>18</sup>C. A. Perottoni and J. A. H. da Jornada, *Science* **280**, 886 (1998); T. R. Ravindran, A. K. Arora, and T. A. Mary, *Phys. Rev. Lett.* **84**, 3879 (2000); B. Chen, D. V. S. Muthu, Z. X. Liu, A. W. Sleight, and M. B. Kruger, *Phys. Rev. B* **64**, 214111 (2001); T. Sakuntala, R. Rao, A. B. Garg, S. N. Achary, and A. K. Tyagi, *J. Appl. Phys.* **104**, 063506 (2008).

<sup>19</sup>S. Carlson and A. M. K. Anderson, *J. Appl. Crystallogr.* **34**, 7 (2001); I. Loa, A. Grzechnik, U. Schwarz, K. Syassen, M. Hanfland, and R. K. Kremer, *J. Alloys Compd.* **317–318**, 103 (2001); U. L. C. Hemamala, F. El-Ghoussein, A. M. Goedken, B. Chen, C. Leroux, and M. B. Kruger, *Phys. Rev. B* **70**, 214114 (2004); T. Sakuntala, A. K. Arora, V. Sivasubramanian, R. Rao, S. Kalavathi, and S. K. Deb, *ibid.* **75**, 174119 (2007).

<sup>20</sup>A. P. Hammersley, S. O. Svensson, M. Hanfland, A. N. Fitch, and D. Hausermann, *High Press. Res.* **14**, 235 (1996).

<sup>21</sup>A. C. Larson and R. B. Von Dreele, GSAS: General Structure Analysis System Los Alamos National Laboratory Report No. LAUR 86–748, 2000 (unpublished).

<sup>22</sup>S. Venugopalan and A. K. Ramdas, *Phys. Rev. B* **5**, 4065 (1972).

<sup>23</sup>S. C. Abrahams, P. B. Jamieson, and A. L. Bernstein, *J. Chem. Phys.* **47**, 4034 (1967).

<sup>24</sup>JCPDS #37–0485.

<sup>25</sup>B. H. Toby, *Powder Diffr.* **21**, 67 (2006).

<sup>26</sup>F. Birch, *J. Geophys. Res.* **83**, 1257 (1978).

<sup>27</sup>S. K. Sikka, *J. Phys. Condens. Matter* **16**, S1033 (2004).

<sup>28</sup>A. L. Goodwin, D. A. Keen, and M. G. Tucker, *Proc. Natl. Acad. Sci. U.S.A.* **105**, 18708 (2008).

<sup>29</sup>V. Milman, B. Winkler, R. H. Nobes, E. V. Akhmatkaya, C. J. Pickard, and J. A. White, *JOM* **52**, 22 (2000).

<sup>30</sup>V. Milman, E. V. Akhmatkaya, R. H. Nobes, B. Winkler, C. J. Pickard, and J. A. White, *Acta Crystallogr. B* **57**, 163 (2001).

<sup>31</sup>K. Papagelis, J. Arvanitidis, G. Kellis, S. Ves, and G. A. Kourouklis, *J. Phys. Condens. Matter* **14**, 3875 (2002).

<sup>32</sup>J. Arvanitidis, K. Papagelis, D. Christofilos, H. Kimura, G. A. Kourouklis, and S. Ves, *Phys. Status Solidi B* **241**, 3149 (2004).

<sup>33</sup>J. D. Jorgensen, Z. Hu, S. Teslic, D. N. Argryriou, S. Short, J. S. O. Evans, and A. W. Sleight, *Phys. Rev. B* **59**, 215 (1999).

<sup>34</sup>J. D. Jorgensen, Z. Hu, S. Short, A. W. Sleight, and J. S. O. Evans, *J. Appl. Phys.* **89**, 3184 (2001).

<sup>35</sup>Y.-M. Ma, H.-Y. Chen, X.-F. Li, L.-L. Gao, Q.-L. Cui, and G.-T. Zou, *Chin. Phys. Lett.* **24**, 1180 (2007).

<sup>36</sup>L. Zhang, H. Ahsbahs, A. Kutoglu, and C. A. Geiger, *Phys. Chem. Miner.* **27**, 52 (1999).

<sup>37</sup>P. R. Stoddart, P. E. Ngoepe, P. M. Mjwara, J. D. Comins, and G. A. Saunders, *J. Appl. Phys.* **73**, 7298 (1993).

<sup>38</sup>H. Hua, S. Mirov, and Y. K. Vohra, *Phys. Rev. B* **54**, 6200 (1996).